High density flux of Co nanoparticles produced by a simple gas aggregation apparatus

G. T. Landi, S. A. Romero, and A. D. Santos
Departamento de Física dos Materiais e Mecânica, Laboratório de Materiais Magnéticos, Instituto de Física, Universidade de São Paulo, Caixa Postal 66318, 05314-970 São Paulo, SP, Brazil

(Received 3 August 2009; accepted 15 February 2010; published online 17 March 2010)

Gas aggregation is a well known method used to produce clusters of different materials with good size control, reduced dispersion, and precise stoichiometry. The cost of these systems is relatively high and they are generally dedicated apparatuses. Furthermore, the usual sample production speed of these systems is not as fast as physical vapor deposition devices posing a problem when thick samples are needed. In this paper we describe the development of a multipurpose gas aggregation system constructed as an adaptation to a magnetron sputtering system. The cost of this adaptation is negligible and its installation and operation are both remarkably simple. The gas flow for flux in the range of 60–130 SCCM (SCCM denotes cubic centimeter per minute at STP) is able to completely collimate all the sputtered material, producing spherical nanoparticles. Co nanoparticles were produced and characterized using electron microscopy techniques and Rutherford back-scattering analysis. The size of the particles is around 10 nm with around 75 nm/min of deposition rate at the center of a Gaussian profile nanoparticle beam. © *2010 American Institute of Physics.* [doi:10.1063/1.3355075]

I. INTRODUCTION

In recent years, novel electronic, magnetic, and optical properties have been observed on nanoparticulate systems made from different materials.[1–3] These properties influence the development of new techniques to produce and manipulate these objects with controllable size distributions and structural properties. Among them, chemical reduction methods[4] and gas aggregation techniques[5] may be mentioned. The first shows greater simplicity and the latter holds the advantage of growing the objects in vacuum, enabling them to be codeposited with dielectric, metallic, or multilayer matrixes. For most of these methods producing thick samples are challenging since long deposition times may be needed. Several applications may involve the preparation of such samples as *p. e.* metallic catalysts[6] or permanent magnets.[7]

In this paper we present the development of a nanoparticle gun (NPG) based on the magnetron sputtering technique and the gas aggregation method.[5,8,9] In general, this kind of equipment operates in ultrahigh vacuum and is devoted to the production of low fluxes of small nanoparticles with fine size control by mass filtering. Here, our intention was to develop a device as easy to operate as the sputtering system itself. Our main motivation is to be able to produce films and multilayers where the nanoparticles are one of the constituents of the sample. From installation to operation, the overall simplicity of the system stands out. Using highly collimated gas fluxes, we are able to obtain deposition rates higher than previously reported on similar systems, even using remarkably low sputtering powers (~30 W). In fact, we observed that nearly all of the material effectively removed from the target is deposited on the substrate. Like other gas aggregation systems, the range of materials suited for usage is vast and matrix codeposition is feasible. In this paper, Co was the element of choice for the nanoparticles.

II. EXPERIMENTAL SETUP

A commercial magnetron sputtering system (ATC 2000 from AJA International) was used and adapted to support the NPG. The sputtering system consists of a high-vacuum chamber with four sputtering guns connected to dc or rf power supplies. The base pressure is around 10^{-7} Torr. The NPG was installed over one of the sputtering guns. It consists of a cylindrical chamber with 10 cm in diameter and 15 cm in length. This chamber is sealed, except for a 2 mm aperture on its extremity (see Fig. 1). The power applied to the target is usually 30 W, a significantly low but in this case appropriate value. A constant flow of Ar is introduced at the bottom part of the gun where the sputtering target resides. Typical values of 85 SCCM (SCCM denotes cubic centimeter per minute at STP) of flux are used. We obtain about 5 mTorr of pressure in the main chamber and 1 Torr in the condensation chamber with both pressures having a linear relation to the gas flux. For around 85 SCCM the Ar flux inside the NPG is supposed to be lamellar. The agglomeration process happens in the usual way, by thermalization with the gas and consequent condensation of the sputtered material. After leaving the aperture, the just grown particles and the argon flux expand aerodynamically toward the substrate placed 1–5 cm from the aperture. Due to the high efficiency of the NPG, the power applied to the target is very low and therefore, it is not necessary to use a cooling system. The installation of the NPG in the multiuser sputtering system takes only a couple of hours and its overall construction cost was negligible.

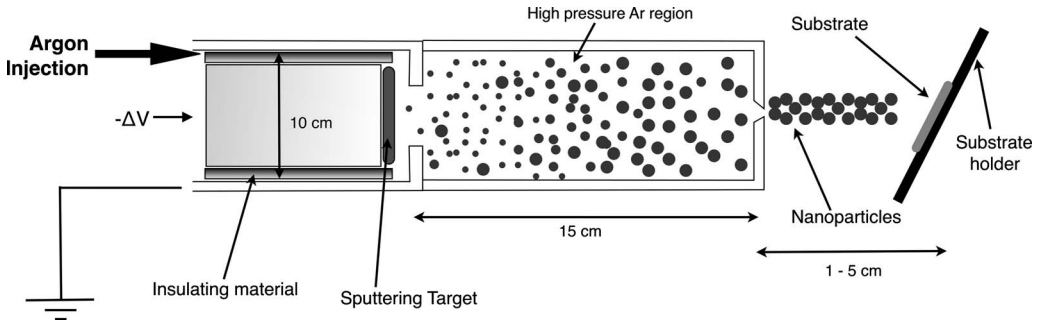

FIG. 1. Schematic diagram of the NPG as an adaptation of a magnetron sputtering gun.

III. THE AGGLOMERATION PROCESS

Due to the geometry of the system, the condensation process inside the NPG happens simultaneously with its collimation of the nanoparticles to the Ar flux. First, concerning the thermalization of the atomic vapor, the typical energies of the atoms being removed from the target are between a few and some tens of eV, which are at least two orders of magnitude larger than the thermal energy of the gas. But, since the Ar/Co mass ratio is around 2/3, only seven to ten collisions are enough to effectively thermalize them.[10] Furthermore, due to the high pressure inside the chamber, the Ar–Co mean free path (λ_{Ar-Co}) is only a few microns. Therefore, still close to the target, the atomic vapor would already be thermalized. But, at the same time, this very short λ_{Ar-Co} implies a high probability of the Co atom to be reabsorbed by the target, corresponding to a strong reduction of the Co flux in relation to the standard sputtering yield. Being thermalized or not, it is reasonable to assume that any Co specimen (atom, dimer, trimer, etc.) will chemically bond to another one in the event of a collision.

Considering 1 Torr of pressure, the effective sputter yield of any material is two or three orders of magnitude smaller than[10] standard sputtering condition[11] at a few mTorr. Taking this into account, from the electric current for 30 W, we are able to estimate the flow of Co atoms in the range from 4×10^{15} to 4×10^{14} atoms/s. This may be translated into a Co–Co mean free path (λ_{Co-Co}) of a few millimeters close to the target. Since the concentration of Co specimens is considerably higher in the beginning of the trajectory, close to the target the condensation speed will also be higher. Therefore, fast aggregation between light Co specimens will occur in the beginning and slower bonds between heavier specimens in the end of the trajectory inside the NPG.

In terms of the gas flow, the higher the Ar pressure, the faster the thermalization. But, if by chance two Co atoms create a dimer before thermalizing, then the thermalization efficiency is greatly reduced. For trimers and so forth, this effect is even more substantial. Therefore, if there are not enough Ar atoms, the atomic vapor will continue condensing but will not have its trajectory collimated to the lamellar Ar flux. Since the initial sputtering direction follows a cosine distribution of material and the aperture at the end of the chamber is small, only an extremely low percentage of particles would leave the chamber with the majority being fixated on the inner walls. But, on the other hand, if the amount of Ar atoms is large, then the atomic vapor will thermalize and will follow the Ar gas along its trajectory, ultimately leaving the aperture and being deposited on the substrate.

In light of these arguments it is possible to conclude that there is a competition between the thermalization and the condensation processes where the thermalization needs to come first in order to collimate the nanoparticles to the Ar flux. This competition is highly nonlinear with an intrinsic threshold in the Ar flux around ~60 SCCM, below which the deposition rates fall abruptly to negligible values. Above 60 SCCM, the deposition rates increases almost linearly. Around 130 SCCM, on the other hand, it reduces abruptly, probably due to turbulent gas state.

The atomic flux for 85 SCCM of Ar is $\sim3\times10^{19}$ atoms/s. Therefore, for 30 W of power, the relative concentration of Co in the chamber is less than 0.01%. With these values, the collimation capabilities of the system are very significant with almost no material seen in the inner walls of the NPG, even after more than 10 h of deposition. This is an indication that almost all the effectively sputtered atoms are deviated from their trajectories, condensed into nanoparticles and deposited on the substrate, which is a remarkable result.

IV. SAMPLE CHARACTERIZATION

For this work, Co NPs were produced using 85 SCCM of Ar flux and 30 W of dc power. The samples were analyzed using high-resolution transmission electron microscopy (HRTEM), scanning electron microscopy (SEM), and Rutherford back-scattering (RBS) analysis. Carbon coated Cu grids were used for HRTEM and Si substrates for SEM/RBS. For the last case the deposition time was 10 min, but for the first one, in order to obtain low concentration of nanoparticles, the substrate holder was rotating and the grid passed in front of the gun only five times.

Figure 2(a) illustrates HRTEM images of the Co nanoparticles with its size distribution histogram [Fig. 2(b)]. The mean diameter obtained by a lognormal fitting is 10.0 nm with 14% of dispersion. On Fig. 2(c) we have the image of only one typical particle where it is possible to see two different crystallographic regions. This illustrates the main characteristic of this production process which is to produce agglomerates of agglomerates. This means that here, what is being called nanoparticles is in fact a cluster of smaller particles. Since the grain size is too small, the particles do not present a clear crystallographic structure as was seen in several x-ray diffraction experiments, not presently shown.

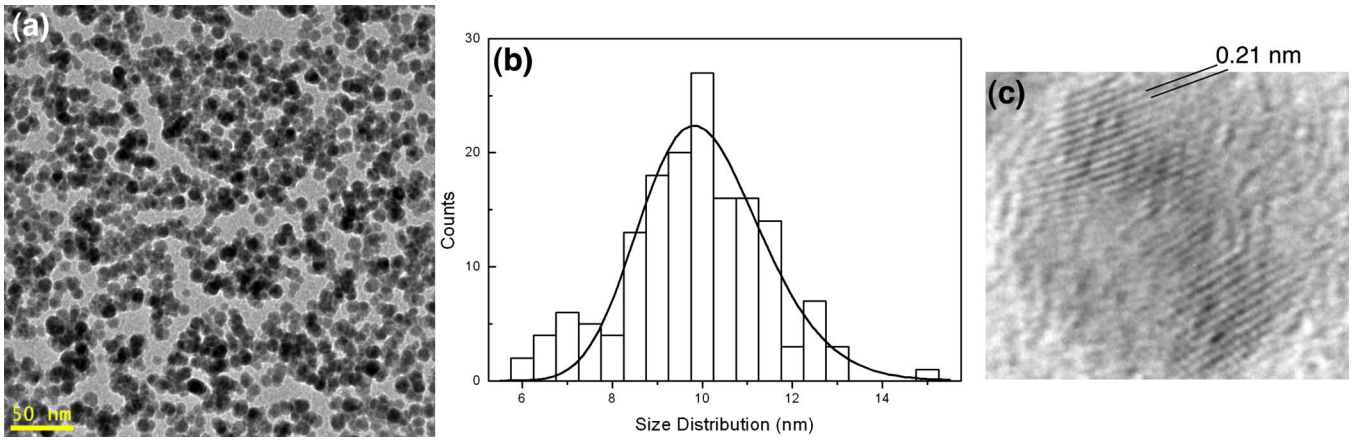

FIG. 2. (Color online) (a) HRTEM image of the Co NPs and (b) its size distribution histogram with a lognormal fitting (line). The calculated mean diameter is (10.0 ± 1.4) nm. (c) HRTEM image of one specific nanoparticle showing different agglomerates.

Figure 3(a) shows five different depositions made on a piece of white paper in function of the distance between the substrate and the gun aperture. The exceptional collimation of the system can be seen as the spot size of the beam increases only slightly as the distance increases from 1 to 5 cm.

Several RBS measurements were performed on a sample along a direction such as the one described by the dashed line over the first stain on Fig. 3(a). The measurements were done using a 0.3 mm wide, 1.4 MeV proton beam. On each spectrum, the simulation of the experimental data gave the atomic density of Co by unit surface. These results were plotted as a function of the position of the irradiation, as shown on Fig. 3(b). It is also shown on this plot, a Gaussian fit with exceptional agreement to the experimental data. The obtained peak value is equivalent to 75 nm/min of Co deposition or, namely, one layer of nanoparticles deposited every 8 s on the center. These values correspond to a 50 fold increase if compared, thickness wise, to a regular sputtering deposition at 100 W of power and 5 mTorr of pressure. The half-height width of the spot is 2.5 mm. Finally, for the RBS numerical simulations we had to consider a roughness of approximately the same thickness as the metallic layer, confirming our expectations that these samples are highly porous. Since the total deposition time was 10 min, the peak of the sample consisted of ~750 nm of particles occupying ~1500 nm of physical space.

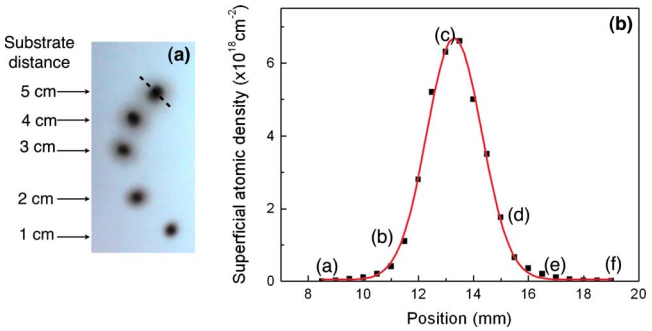

FIG. 3. (Color online) (a) View of five depositions of Co nanoparticles in function of the distance between the substrate and the aperture of the gun. The dashed line on the upper most deposition corresponds to the direction that the RBS measurements made. (b) The superficial atomic density obtained from RBS in function of the position over the sample. The continuous line corresponds to a Gaussian fitting on the experimental data. The letters on the graph are reference to Fig. 4.

Integrating over the Gaussian distribution of Fig. 3(b) and taking into account the deposition time, we were able to obtain the flux of atoms deposited on the substrate per second as 7×10^{14} atoms/s. This value may be directly compared to the range of $4 \times 10^{15} - 4 \times 10^{14}$ atoms/s estimated as the initial Co atoms flux being removed from the target. The agreement between these two numbers is extremely good and offers another indication that almost all the material being removed from the sputtering target ends up as nanoparticles on the substrate.

On the same sample where the RBS measurements were done, several SEM images have been obtained on different regions, marked by letters in Fig. 3(b). These images are shown in Fig. 4. The goal of these measurements was to visualize the concentration of material on the different regions of the substrate. It is clear the quite homogeneous distribution of the agglomerates and the highly porous behavior of the sample. Furthermore, on images (a) and (f) of Fig. 4, which represent the areas with low density of material, RBS measurements gave around 6 nm for the effective thickness. This value is compatible with less than one filled layer of spherical 10 nm nanoparticles showing that there is good compatibility between both analyses.

Bearing in mind that the material used and the size of the particles greatly influence the deposition rates, our results can be compared to other systems, even considering that all of them are very geometry-sensitive. In the system presented by Baker *et al.* in 2000,[8] values on the order of 0.01 nm/min were typically shown, but concerning particles with smaller sizes and narrower size distributions. The system used by Sellmyer *et al.*[9] shows typical values of 18 nm/min. Both of them refer to Fe or Fe alloys whose sputtering yields are similar to Co. Koch *et al.*[12] present maximum values of about 30 nm/min, but for Cu, sputtering yield is twice that of Co. Finally, it is important to emphasize that all these systems have used over 100 W as the sputtering power.

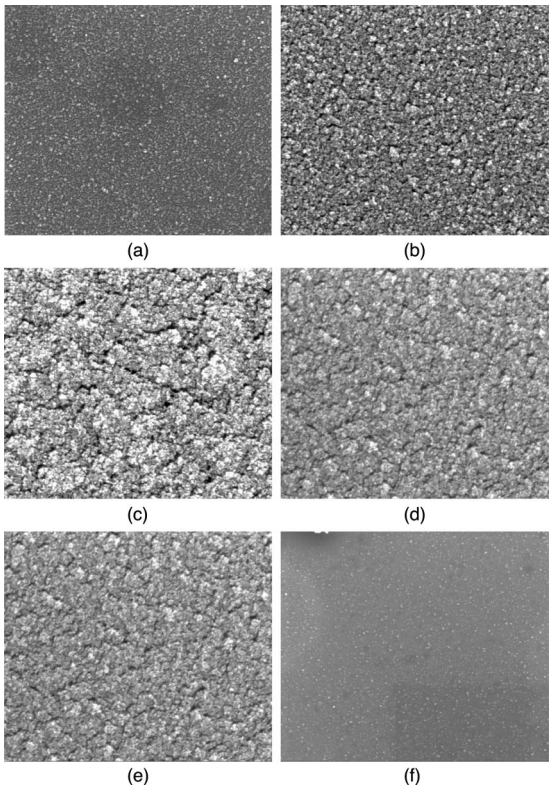

FIG. 4. SEM images of Co NPs for the positions [(a)–(f)] on the Fig. 3(b).

V. CONCLUSIONS

In conclusion, we have described in this paper the development of an extremely simple and cheap NPG constructed as an easy-to-install adaptation to an already operational magnetron sputtering system. Even with its simplicity, we were able to produce 10 nm Co nanoparticles with 14% dispersion without using any kind of mass filtering systems. We obtained that the dependence on the deposition rates as a function of the gas flow is highly nonlinear and that for the range between 60 and 130 SCCM, the gas is able to collimate the flow of particles in a way that almost all the material removed from the target is deposited on the substrate. Therefore, even with low sputtering powers, we are able to produce samples with speeds over 50 times higher than regular magnetron sputtering depositions.

ACKNOWLEDGMENTS

This work was supported by the Brazilian Agencies CNPq and FAPESP. We acknowledge the Laboratório de Microscopia Eletrônica, Centro de Ciência e Tecnologia de Materiais—CCTM/IPEN for the HRTEM measurements.

[1] M. Behboudnia and P. Sen, Phys. Rev. B **63**, 035316 (2001).
[2] S. Sun, C. B. Murray, D. Weller, L. Folks, and A. Moser, Science **287**, 1989 (2000).
[3] K. Lindfors, T. Kalkbrenner, P. Stoller, and V. Sandoghdar, Phys. Rev. B **93**, 037401 (2004).
[4] Y. Xia, Y. Xiong, B. Lim, and S. E. Skrabalak, Angew. Chem., Int. Ed. **48**, 60 (2009).
[5] J. Mühlbach, E. Recknagel, and K. Sattler, Surf. Sci. **106**, 188 (1981).
[6] D. Phokharatkul, Y. Ohno, H. Nakano, S. Kishimoto, and T. Mizutani, Appl. Phys. Lett. **93**, 053112 (2008).
[7] A. Moser, K. Takano, D. T. Margulies, M. Albrecht, Y. Sonobe, Y. Ikeda, S. Sun, and E. E. Fullerton, J. Phys. D **35**, R157 (2002).
[8] S. H. Baker, S. C. Thornton, K. W. Edmonds, M. J. Maher, C. Norris, and C. Binns, Rev. Sci. Instrum. **71**, 3178 (2000).
[9] Y. Xu, Z. G. Sun, Y. Qiang, and D. J. Sellmyer, J. Appl. Phys. **93**, 8289 (2003).
[10] R. S. Mason and M. Pichilingi, J. Phys. D **27**, 2363 (1994).
[11] A. J. Stirling and W. D. Westwood, J. Phys. D **4**, 246 (1971).
[12] S. A. Koch, G. Palasantzas, T. Vystavel, and J. T. M. De Hosson, Phys. Rev. B **71**, 085410 (2005).